

Asymmetric Sandwich-Type Polyoxoanions. Synthesis, Characterization, and X-ray Crystal Structures of Diferric Complexes $[\text{TM}^{\text{II}}\text{Fe}^{\text{III}}_2(\text{P}_2\text{W}_{15}\text{O}_{56})(\text{P}_2\text{TM}^{\text{II}}\text{W}_{13}\text{O}_{52})]^{16-}$, TM = Cu or Co

Travis M. Anderson, Kenneth I. Hardcastle, Nelya Okun, and Craig L. Hill*

Department of Chemistry, Emory University, Atlanta, Georgia 30322

Received May 21, 2001

Reaction of the diferric sandwich-type polyoxometalate $(\text{NaOH})_2\text{Fe}^{\text{III}}_2(\text{P}_2\text{W}_{15}\text{O}_{56})^{16-}$ (**1**) with excess aqueous Cu(II) or Co(II) yields a new type of d-electron-metal substituted polyoxometalate, $[\text{TM}^{\text{II}}\text{Fe}^{\text{III}}_2(\text{P}_2\text{W}_{15}\text{O}_{56})(\text{P}_2\text{TM}^{\text{II}}\text{W}_{13}\text{O}_{52})]^{16-}$, TM = Cu (**2**), Co (**3**), respectively. The structure of the sodium salt of **2** (Na**2**), determined by single-crystal X-ray diffraction analysis ($a = 13.4413(9)$ Å, $b = 21.2590(15)$ Å, $c = 25.5207(18)$ Å, $\alpha = 80.475(2)^\circ$, $\beta = 85.555(2)^\circ$, $\gamma = 89.563(2)^\circ$, triclinic, $P\bar{1}$, $R_1 = 5.42\%$, based on 43097 independent reflections), consists of a defect Fe_2Cu central unit sandwiched between two different trivacant Wells–Dawson-type units, P_2W_{15} and $\text{P}_2\text{Cu}_2\text{W}_{13}$, where the latter unit has two octahedral Cu(II) ions substituted for two adjacent belt W(VI) atoms. The CuO_5OH_2 octahedron in the central unit shows pronounced Jahn–Teller distortion. A low-resolution X-ray structure of Na**3** is included in the Supporting Information. UV–visible, infrared, ^{31}P NMR, cyclic voltammetric, and elemental analysis data are all consistent with the structure determined from the X-ray analysis. Cyclic voltammograms of **2** and **3** exhibit multiple electron-transfer processes under ambient conditions, and copper or cobalt incorporation into the framework of **1** results in a substantial perturbation of the electrochemical properties of the polyoxotungstate framework. The tetra-*n*-butylammonium salts of **2** and **3** (readily prepared by metathesis) are stable and effective catalysts for the oxidation of some alkenes with high yields based on H_2O_2 .

Introduction

Polyoxometalates^{1–3} (POMs for convenience) and their transition metal substituted derivatives (TMSPs) are a large class of highly modifiable metal–oxygen anionic clusters that facilitate a range of basic studies (from electron transfer^{4,5} and ion pairing^{6–10} to self-assembly^{11,12}) as well as applied studies.¹³ Given the importance of precise compositions and structures in all investigations centered around this large and growing class of clusters, the continuing development of rational methods for the systematic modification of POM systems remains very important. A significant subset of this entails methods for the site selective substitution of addenda atoms that form the frameworks of POM structures.

Metal incorporation (substitution or addition) involves not only control of incorporation of d-metal centers but also maintenance of the overall POM structure (inter-subunit connectivities) during such processes.¹⁴ Tézé, Hervé, and co-

- (1) Pope, M. T. *Heteropoly and Isopoly Oxometalates*; Springer-Verlag: Berlin, 1983.
- (2) Hill, C. L.; Prosser-McCartha, C. M. *Coord. Chem. Rev.* **1995**, *143*, 407–455.
- (3) Hill, C. L., Guest Ed. *Chem. Rev.* **1998**, *98*, 1–389.
- (4) (a) Kozik, M.; Baker, L. C. W. *J. Am. Chem. Soc.* **1990**, *112*, 7604–7611. (b) Kozik, M.; Baker, L. C. W. In *Polyoxometalates: From Platonic Solids to Anti-retroviral Activity*; Pope, M. T., Müller, A., Eds.; Kluwer Academic Publishers: Dordrecht, 1994; pp 191–202.
- (5) Weinstock, I. A. *Chem. Rev.* **1998**, *98*, 113–170.
- (6) Day, V. W.; Klemperer, W. G.; Maltbie, D. J. *J. Am. Chem. Soc.* **1987**, *109*, 2991–3002.
- (7) Kirby, J. F.; Baker, L. C. W. *Inorg. Chem.* **1998**, *37*, 5537–5543.
- (8) Grigoriev, V. A.; Hill, C. L.; Weinstock, I. A. *J. Am. Chem. Soc.* **2000**, *122*, 3544–3545.
- (9) Grigoriev, V. A.; Cheng, D.; Hill, C. L.; Weinstock, I. A. *J. Am. Chem. Soc.* **2001**, *123*, 5292–5307.
- (10) Anderson, T. M.; Hill, C. L. *Inorg. Chem.*, submitted.
- (11) Müller, A.; Peters, F.; Pope, M. T.; Gatteschi, D. *Chem. Rev.* **1998**, *98*, 239–272.
- (12) Müller, A.; Das, S. K.; Kogerler, P.; Bogge, H.; Schmidtman, M.; Trautwein, A. X.; Schunemann, V.; Krickemeyer, E.; Preetz, W. *Angew. Chem., Int. Ed.* **2000**, *39*, 3414–3417 and references therein.

- (13) Applications of polyoxometalates range from catalysis ((a) Hill, C. L.; Prosser-McCartha, C. M. *Coord. Chem. Rev.* **1995**, *143*, 407–455. (b) Okuhara, T.; Mizuno, N.; Misono, M. *Adv. Catal.* **1996**, *41*, 113–252. (c) Mizuno, N.; Misono, M. *Chem. Rev.* **1998**, *98*, 199–218. (d) Kozhevnikov, I. V. *Chem. Rev.* **1998**, *98*, 171–198. (e) Neumann, R. *Prog. Inorg. Chem.* **1998**, *47*, 317–370. (f) Katsoulis, D. E. *Chem. Rev.* **1998**, *98*, 359–388) and materials chemistry ((g) Coronado, E.; Gómez-García, C. J. *Chem. Rev.* **1998**, *98*, 273–296. (h) Zeng, H.; Newkome, G. R.; Hill, C. L. *Angew. Chem., Int. Ed.* **2000**, *39*, 1771–1774. (i) Klemperer, W. G.; Wall, C. G. *Chem. Rev.* **1998**, *98*, 297–306. (j) Müller, A.; Das, S. K.; Bogge, H.; Schmidtman, M.; Botar, A.; Patrut, A. *Chem. Commun.* **2001**, 657–658. (k) Müller, A.; Das, S. K.; Kuhlmann, C.; Bogge, H.; Schmidtman, M.; Diemann, E.; Krickemeyer, E.; Hormes, J.; Modrow, H.; Schindler, M. *Chem. Commun.* **2001**, 655–656. (l) Kurth, D. G.; Lehmann, P.; Volkmer, D.; Colfen, H.; Koop, M. J.; Müller, A.; Du Chesne, A. *Chem. Eur. J.* **2000**, *6*, 385–393. (m) Kurth, D. G.; Lehmann, P.; Volkmer, D.; Müller, A.; Schwahn, D. *J. Chem. Soc., Dalton Trans.* **2000**, 3989–3998) to medicine ((n) Judd, D. A.; Nettles, J. H.; Nevins, N.; Snyder, J. P.; Liotta, D. C.; Tang, J.; Ermolieff, J.; Schinazi, R. F.; Hill, C. L. *J. Am. Chem. Soc.* **2001**, *123*, 886–897. (o) Rhule, J. T.; Hill, C. L.; Judd, D. A.; Schinazi, R. F. *Chem. Rev.* **1998**, *98*, 327–357. (p) Yamase, T. In *Polymeric Materials Encyclopedia*; Salamone, J. C., Ed.; CRC Press: Boca Raton, 1996; pp 365–373).
- (14) Metal incorporation is closely related to ion pairing in POMs, a phenomenon recently probed from the structural perspective ((a) Day, V. W.; Klemperer, W. G.; Maltbie, D. J. *J. Am. Chem. Soc.* **1987**, *109*, 2991–3002. (b) Kirby, J. F.; Baker, L. C. W. *Inorg. Chem.* **1998**, *37*, 5537–5543. (c) Knoth, W. H.; Harlow, R. L. *J. Am. Chem. Soc.* **1981**, *103*, 1865–1867. (d) Contant, R.; Tézé, A. *Inorg. Chem.* **1985**, *24*, 4610–4614), and from the dynamic and spectroscopic perspectives ((e) Grigoriev, V. A.; Hill, C. L.; Weinstock, I. A. *J. Am. Chem. Soc.* **2000**, *122*, 3544–3545. (f) Grigoriev, V. A.; Cheng, D.; Hill, C. L.; Weinstock, I. A. *J. Am. Chem. Soc.* **2001**, *123*, 5293–5307. (g) Anderson, T. M.; Hill, C. L. *Inorg. Chem.*, submitted).

workers have developed techniques involving stable alkali metal complexes of various Keggin derivatives for site-specific substitution in the polyoxotungstate framework.^{15,16} Through the stereospecific preparation of the lacunary species, these investigators were able to control the site of metal substitution. Contant and co-workers have reported systematic preparations of molybdenum- and vanadium-substituted derivatives of α - $P_2W_{18}O_{62}^{6-}$, a Wells–Dawson POM studied from both the synthetic and dynamic perspectives.^{10,17,18} This work seeks to develop complementary methods to control the site of substitution in other classes of POMs. Specifically, we examine the effects of cap isomerization on substitution patterns in sandwich-type polyoxometalates, a growing and particularly versatile subclass of POMs.

Sandwich-type POMs are formed by the reaction of transition metal cations with one of two general types of trivalent lacunary POMs.^{19–40} The A-type is formed by removing one corner-sharing WO_6 octahedron from each of three bridging W_3O_{13} triads; the B-type is formed by removal of one entire W_3O_{13} triad. Each trivalent lacunary POM yields a different type of sandwich structure (Figure 1). In previous reports, the junctions between the trivalent lacunary species and the central tetrameric unit were β for all known B-type Keggin- or Wells–Dawson-derived tetranuclear sandwich complexes in a manner analogous

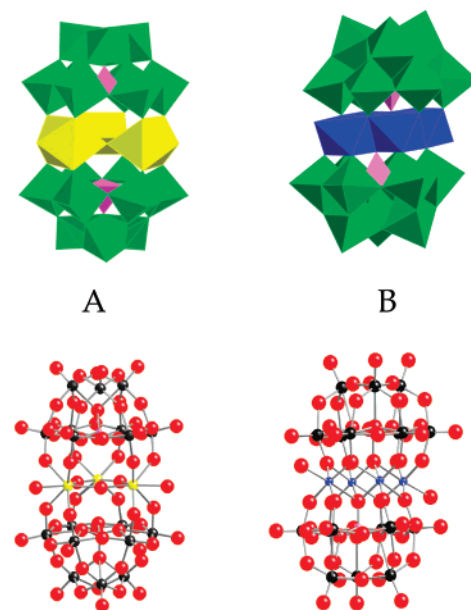


Figure 1. Polyhedral and ball-and-stick representations (top to bottom) of the most common sandwich-type polyoxometalates derived from different trivalent lacunary Keggin-type structures: (A) A-type sandwich; (B) B-type sandwich.

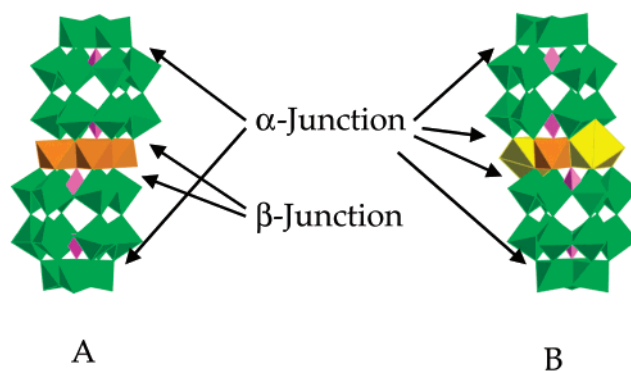


Figure 2. Polyhedral representations of isomers of the Wells–Dawson-type sandwich structures: (A) traditional β -sandwich structure; (B) new α -sandwich structure described in this article.

to Baker–Figgis (cap rotation) isomers (Figure 2A). Recently, however, a sandwich-type POM with α -junctions between the trivalent lacunary species was reported, $(NaOH)_2Fe^{III}_2(P_2W_{15}O_{56})_2$, **1** (Figure 2B).⁴⁰ This complex contained the Fe_2O_2 motif prevalent in several redox metalloenzymes.⁴¹ The tetra-*n*-butylammonium salt catalyzes the selective epoxidation of alkenes with H_2O_2 under ambient conditions.⁴²

We report here that **1** reacts with hydrated first-row transition metal cations to form a new family of mixed-metal diiron-containing sandwich-type POMs of formula $[TM^II Fe^{III}_2(P_2W_{15}O_{56})(P_2TM^II W_{13}O_{52})]^{16-}$, TM = Cu (**2**), Co (**3**). Like the Keggin-type polytungstozincate sandwich POMs first prepared by Tourné and co-workers,³⁴ these compounds contain two different species in the central unit. Two tungsten atoms, located in the adjacent belt region (nearest the vacant site in the central unit), are now replaced by first-row transition metals with retention of the interunit connection isomerism at the site of metal incorporation, thereby creating the first sandwich-type POMs that are asymmetric based on metal substitution in the POM units. In addition, these complexes exhibit metal incorporation into two adjacent belt positions (generally referred to as α_1 positions in Wells–Dawson structures) without accompanying replacement of cap-position tungsten atoms, chem-

- (15) Canny, J.; Tézé, A.; Thouvenot, R.; Hervé, G. *Inorg. Chem.* **1986**, *25*, 2114–2119.
- (16) Tézé, A.; Hervé, G. In *Inorganic Syntheses*; Ginsberg, A. P., Ed.; John Wiley and Sons: New York, 1990; Vol. 27, pp 85–135.
- (17) Contant, R.; Ciabrini, J. P. *J. Inorg. Nucl. Chem.* **1981**, *43*, 1525–1528.
- (18) Abbessi, M.; Contant, R.; Thouvenot, R.; Hervé, G. *Inorg. Chem.* **1991**, *30*, 1695–1702.
- (19) Weakley, T. J. R.; Finke, R. G. *Inorg. Chem.* **1990**, *29*, 1235–1241.
- (20) Khenkin, A. M.; Hill, C. L. *Mendeleev Commun.* **1993**, 140–141.
- (21) Zhang, X.; Chen, Q.; Duncan, D. C.; Campana, C.; Hill, C. L. *Inorg. Chem.* **1997**, *36*, 4208–4215.
- (22) Gómez-García, C. J.; Borrás-Almenar, J. J.; Coronado, E.; Ouahab, L. *Inorg. Chem.* **1994**, *33*, 4016–4022.
- (23) Finke, R. G.; Weakley, T. J. R. *J. Chem. Crystallogr.* **1994**, *24*, 123–128.
- (24) Bi, L.-H.; Wang, E.-B.; Peng, J.; Huang, R.-D.; Xu, L.; Hu, C.-W. *Inorg. Chem.* **2000**, *39*, 671–679.
- (25) (a) Finke, R. G.; Droegge, M. W. *Inorg. Chem.* **1983**, *22*, 1006–1008. (b) Finke, R. G.; Droegge, M. W.; Domaille, P. J. *Inorg. Chem.* **1987**, *26*, 3886–3896.
- (26) Zhang, X.; Chen, Q.; Duncan, D. C.; Lachicotte, R. J.; Hill, C. L. *Inorg. Chem.* **1997**, *36*, 4381–4386.
- (27) Weakley, T. J. R.; Evans, H. T., Jr.; Showell, J. S.; Tourné, G. F.; Tourné, C. M. *J. Chem. Soc., Chem. Commun.* **1973**, 139–140.
- (28) Finke, R. G.; Droegge, M.; Hutchinson, J. R.; Gansow, O. *J. Am. Chem. Soc.* **1981**, *103*, 1587–1589.
- (29) Gómez-García, C. J.; Coronado, E.; Gómez-Romero, P.; Casañ-Pastor, N. *Inorg. Chem.* **1993**, *32*, 3378–3381.
- (30) Zhang, X. Y.; Jameson, G. B.; O'Connor, C. J.; Pope, M. T. *Polyhedron* **1996**, *15*, 917–922.
- (31) Evans, H. T.; Tourné, C. M.; Tourné, G. F.; Weakley, T. J. R. *J. Chem. Soc., Dalton Trans.* **1986**, 2699–2705.
- (32) Wasfi, S. H.; Rheingold, A. L.; Kokoszka, G. F.; Goldstein, A. S. *Inorg. Chem.* **1987**, *26*, 2934–2939.
- (33) Casañ-Pastor, N.; Bas-Serra, J.; Coronado, E.; Pourroy, G.; Baker, L. C. W. *J. Am. Chem. Soc.* **1992**, *114*, 10380–10383.
- (34) Tourné, C. M.; Tourné, G. F.; Zonneville, F. *J. Chem. Soc., Dalton Trans.* **1991**, 143–155.
- (35) Kortz, U.; Isber, S.; Dickman, M. H.; Ravot, D. *Inorg. Chem.* **2000**, *39*, 2915–2922.
- (36) Rusu, M.; Marcu, G.; Rusu, D.; Rosu, C.; Tomsa, A.-R. *J. Radioanal. Nucl. Chem.* **1999**, *242*, 467–472.
- (37) Craciun, C.; David, L.; Rusu, D.; Rusu, M.; Cozar, O.; Marcu, G. *J. Radioanal. Nucl. Chem.* **2001**, *247*, 307–310.
- (38) Knoth, W. H.; Domaille, P. J.; Farlee, R. D. *Organometallics* **1985**, *4*, 62–68.
- (39) Knoth, W. H.; Domaille, P. J.; Harlow, R. L. *Inorg. Chem.* **1986**, *25*, 1577–1584.
- (40) Zhang, X.; Anderson, T. M.; Chen, Q.; Hill, C. L. *Inorg. Chem.* **2001**, *40*, 418–419.

istry illustrated by hexavacant P_2W_{12} species. Finally, there is a vacancy left in the central unit (effectively creating an M_3 central unit) in which one could envision incorporation of other organometallic (e.g., SnR_3^-), organic, or inorganic centers.^{43–45} Complete characterization of these complexes by FTIR, UV–visible, ^{31}P NMR, magnetic susceptibility, and X-ray crystallography clearly defines their electronic and structural properties. Cyclic voltammograms of **2** and **3** show that these complexes undergo multiple electron-transfer processes under ambient conditions, and catalytic studies of the tetra-*n*-butylammonium salts of **2** and **3** show that both are effective catalysts for epoxidation by H_2O_2 .

Experimental Section

General Methods and Materials. $\alpha-Na_{12}[P_2W_{15}O_{56}] \cdot 18H_2O$ was prepared according to literature methods.^{25,46} Acetonitrile and other solvents (Aldrich) were used as received. The alkenes were reagent grade from Fluka or Aldrich, and purity was checked by gas chromatography (GC). C, H, and N analyses were performed by Atlantic Microlab Inc., Norcross, GA. Co, Cu, Fe, P, and W analyses were performed by LBB2 Analytical Services Laboratory in Pullman, WA, and Desert Analytics Laboratory in Tucson, AZ. The alkene products were identified by gas-chromatography–mass spectrometry (GC/MS; Hewlett-Packard 5890 series II gas chromatograph coupled with a Hewlett-Packard 5971A mass selective detector) and quantified by GC (Hewlett-Packard 6890 gas chromatograph fitted with a flame ionization detector, a 25 m \times 0.2 mm 5% phenyl methyl silicone capillary column, nitrogen carrier gas, and a Hewlett-Packard 6890 series integrator). Infrared spectra (2% sample in KBr) were recorded on a Nicolet 510 FTIR instrument. The electronic absorption spectra were taken on a Hewlett-Packard 8452A UV/visible spectrophotometer. ^{31}P NMR measurements were made on a Varian Unity 600 MHz spectrometer

using 85% H_3PO_4 in D_2O as an external reference; peak widths (fwhm) are given in hertz. Average magnetic susceptibilities were measured on a Johnson Matthey model MSB-1 magnetic susceptibility balance as neat powders at 24 °C; the balance was calibrated using $Hg[Co(SCN)_4]$ as a standard. The diamagnetic corrections not only were evaluated using Pascal's constants but also were measured using the diamagnetic parent complex, $\alpha-Na_{12}[P_2W_{15}O_{56}] \cdot 18H_2O$. Electrochemical measurements were performed with an EG & G Princeton Applied Research model VersaStat II potentiostat under computer control (Power CV programs) in a conventional three-electrode cell with working glassy carbon, auxiliary Pt, and reference Ag, AgCl/saturated KCl electrodes at ambient temperature. The GC electrode was polished with 0.3 μm $\alpha-Al_2O_3$ powder and rinsed with deionized water before each use. Cyclic voltammograms of 5×10^{-4} M POM in the range from +0.8 to –1.0 V were obtained in 1.0 M aqueous NaCl solutions at pH = 5.0 (acetate buffer) and at scan rates from 50 to 200 mV/s. A background correction (from a solution containing 1 M NaCl only) was subtracted from the cyclic voltammograms to obtain the Faradaic component. Solutions were deaerated with Ar for 15 min before measurements and kept under a positive pressure at all times.

Synthesis of the Sodium Salt of $Cu^{II}(OH)_2Fe^{III}_2(P_2W_{15}O_{56})(P_2Cu^{II}_2(OH)_2W_{15}O_{52})^{16-}$ (Na2). The sandwich-type TMSP compound $[Fe^{III}_2(NaOH)_2(P_2W_{15}O_{56})_2]$, **1** (0.750 g, 0.0825 mmol), was dissolved in a minimal amount of 0.5 M NaCl by gentle heating (50 °C). The solution was cooled to room temperature, and $CuCl_2 \cdot 2H_2O$ (0.141 g, 0.825 mmol) was slowly added to the solution and vigorously stirred for approximately 10 min. A slight color change in the solution (from green to greenish-yellow) was observed after a few minutes. After approximately 7 days, a light yellow amorphous precipitate formed. The solution was filtered and the precipitate redissolved in 0.5 M NaCl. Diffraction quality crystals formed after the solution had stood exposed to the air for 14 days (0.45 g, yield 65%). IR (2% KBr pellet, 1300–400 cm^{-1}): 1088 (s), 1062 (w, sh), 1015 (w, sh), 944 (s), 908 (m), 881 (m), 831 (m), 779 (w), 740 (w), 690 (w), 521 (m), and 488 (w). ^{31}P NMR (9 mM solution in D_2O): two peaks for two symmetry-inequivalent distal P atoms at –10.0 ($\Delta\nu_{1/2} = 350$ Hz) and –11.2 ppm ($\Delta\nu_{1/2} = 300$ Hz). Magnetic susceptibility: $\mu_{eff} = 9.9 \mu_B/mol$ at 297 K. Anal. Calcd for $H_{74}Cu_3Fe_2Na_{16}O_{145}P_4W_{28}$: Cu, 2.27; Fe, 2.00; Na, 4.38; P, 1.48; W, 61.35. Found: Cu, 2.32; Fe, 1.94; Na, 4.41; P, 1.43; W, 61.07. MW: 8390.2.

Tetra-*n*-butylammonium Salt (TBA2). Na2 (0.3 g, 0.035 mmol) was dissolved in 20 mL of H_2O and adjusted to pH = 4 by careful addition of 1 M HCl. Tetra-*n*-butylammonium (TBA) chloride (0.16 g, 0.57 mmol) was added with stirring. To the cloudy yellow solution was added 250 mL of CH_2Cl_2 . The mixture was shaken in a separatory funnel to afford an almost colorless upper aqueous phase and a clear yellow lower organic layer. The organic layer was collected in a round-bottom flask and concentrated using a rotary evaporator. A yellow solid was then precipitated from the concentrated organic layer by addition of diethyl ether (ca. 100 mL). The solid was dried under vacuum for 24 h and redissolved in a minimal amount (ca. 3 mL) of CH_2Cl_2 . An excess amount of diethyl ether was added to give a light yellow solid (0.33 g, yield 80%). The spectroscopic properties establish that **2** had not changed during the conversion of Na2 to TBA2. IR (2% KBr pellet, 1300–400 cm^{-1}): 1151 (w), 1087 (s), 1049 (w, sh), 1014 (w, sh), 947 (s), 911 (m), 888 (m), 824 (m), 786 (m), 749 (w), 696 (s), 528 (m), and 480 (w). ^{31}P NMR (9 mM solution in CD_3CN): two peaks for two symmetry-inequivalent distal P atoms at –7.8 ($\Delta\nu_{1/2} = 350$ Hz) and –9.1 ppm ($\Delta\nu_{1/2} = 320$ Hz). Anal. Calcd for $C_{256}H_{584}Cu_3Fe_3N_{16}O_{112}P_4W_{28}$: C, 27.32; H, 5.23; Cu, 1.69; Fe, 0.99; N, 1.99; P, 1.10; W, 45.74. Found: C, 27.73; H, 5.34; Cu, 1.76; Fe, 1.03; N, 2.03; P, 1.07; W, 46.01. MW: 11253.52.

Synthesis of the Sodium Salt $Co^{II}(OH)_2Fe^{III}_2(P_2W_{15}O_{56})(P_2Co^{II}_2(OH)_2W_{15}O_{52})^{16-}$ (Na3). Complex **1** (0.750 g, 0.0825 mmol) was dissolved in a minimal amount of 0.5 M NaCl. $Co(NO_3)_2 \cdot 6H_2O$ (0.250 g, 0.825 mmol) was slowly added as a powder to the solution and gently heated at 60 °C for ca. 10 min. A slight color change in the solution (from dark red to reddish brown) was observed upon heating. After approximately 7 days, a reddish-brown precipitate formed and was recrystallized as described above for Na2 (0.30 g, yield 43%). IR (2% KBr pellet, 1300–400 cm^{-1}): 1087 (s), 1059 (w, sh), 1017 (w, sh),

- (41) Representative studies of non-heme Fe complexes to model the active site in enzymes such as MMO: (a) Kurtz, D. M., Jr. *Chem. Rev.* **1990**, *90*, 585–606. (b) Sheu, C.; Richert, S. A.; Cofre, P.; Ross, B.; Sobkowiak, A.; Sawyer, D. T.; Kanofsky, J. R. *J. Am. Chem. Soc.* **1990**, *112*, 1936–1942. (c) Fish, R. H.; Konings, M. S.; Oberhausen, K. J.; Fong, R. H.; Yu, W. M.; Christou, G.; Vincent, J. B.; Coggin, D. K.; Buchanan, R. M. *Inorg. Chem.* **1991**, *30*, 3002–3006. (d) Nam, W.; Ho, R.; Valentine, J. S. *J. Am. Chem. Soc.* **1991**, *113*, 7052–7054. (e) Stassinopoulos, A.; Schulte, G.; Papaefthymiou, G. C.; Caradonna, J. P. *J. Am. Chem. Soc.* **1991**, *113*, 8686–8697. (f) Ménage, S.; Vincent, J. M.; Lambeaux, C.; Chottard, G.; Grand, A.; Fontecave, M. *Inorg. Chem.* **1993**, *32*, 4766–4773. (g) Rosenzweig, A. C.; Lippard, S. J. *Acc. Chem. Res.* **1994**, *27*, 229–236. (h) Kim, J.; Harrison, R. G.; Kim, C.; Que, L., Jr. *J. Am. Chem. Soc.* **1996**, *118*, 4373–4379. (i) Que, L., Jr.; Lawrence, Ho, R. Y. N. *Chem. Rev.* **1996**, *96*, 2607–2624. (j) Nguyen, C.; Guajardo, R. J.; Mascharak, P. K. *Inorg. Chem.* **1996**, *35*, 6273–6281. (k) Shu, L.; Nesheim, J. C.; Kauffmann, K.; Münck, E.; Lipscomb, J. D.; Que, L., Jr. *Science* **1997**, *275*, 515–518. (l) Lipscomb, J. D.; Que, L., Jr. *J. Biol. Inorg. Chem.* **1998**, *3*, 331–336. (m) Willems, J.-P.; Valentine, A. M.; Gurbiel, R.; Lippard, S. J. *J. Am. Chem. Soc.* **1998**, *120*, 9410–9416. (n) Valentine, A. M.; Stahl, S. S.; Lippard, S. J. *J. Am. Chem. Soc.* **1999**, *121*, 3876–3887. (o) Payne, S. C.; Hagen, K. S. *J. Am. Chem. Soc.* **2000**, *122*, 6399–6410. (p) Whittington, D. A.; Sazinsky, M. H.; Lippard, S. J. *J. Am. Chem. Soc.* **2001**, *123*, 1794–1795.
- (42) The metal-substituted Zn Tourné complexes developed by Neumann and co-workers are among the most effective sandwich-type POMs for the epoxidation of alkenes ((a) Neumann, R.; Gara, M. *J. Am. Chem. Soc.* **1994**, *116*, 5509–5510. (b) Neumann, R.; Gara, M. *J. Am. Chem. Soc.* **1995**, *117*, 5066–5074. (c) Neumann, R.; Khenkin, A. M. *Inorg. Chem.* **1995**, *34*, 5753–5760. (d) Neumann, R.; Juwiler, D. *Tetrahedron* **1996**, *52*, 8781–8788. (e) Neumann, R.; Khenkin, A. M. *J. Mol. Catal. A: Chem.* **1996**, *114*, 169–180. (f) Neumann, R.; Khenkin, A. M.; Juwiler, D.; Miller, H.; Hara, M. *J. Mol. Catal. A: Chem.* **1997**, *117*, 169–183).
- (43) Chorghade, G. S.; Pope, M. T. *J. Am. Chem. Soc.* **1987**, *109*, 5134–5138.
- (44) Xin, F.; Pope, M. T.; Long, G. J.; Russo, U. *Inorg. Chem.* **1996**, *35*, 1207–1213.
- (45) Xin, F. B.; Pope, M. T. *Organometallics* **1994**, *13*, 4881–4886.
- (46) Contant, R. In *Inorganic Syntheses*; Ginsberg, A. P., Ed.; John Wiley and Sons: New York, 1990; Vol. 27, pp 104–111.

944 (s), 917 (m), 877 (m), 836 (m), 784 (w), 750 (w), 702 (w), 522 (m), and 486 (w). ^{31}P NMR (9 mM solution in D_2O): two peaks for two symmetry-inequivalent distal P atoms at -10.2 ($\Delta\nu_{1/2} = 130$ Hz) and -16.5 ppm ($\Delta\nu_{1/2} = 75$ Hz). Magnetic susceptibility: $\mu_{\text{eff}} = 11.7$ μ_{B} /mol at 297 K. Anal. Calcd for $\text{H}_{74}\text{Co}_3\text{Fe}_2\text{Na}_{16}\text{O}_{145}\text{P}_4\text{W}_{28}$: Co, 2.27; Fe, 1.44; Na, 4.73; P, 1.59; W, 66.20. Found: Co, 2.32; Fe, 1.37; Na, 4.85; P, 1.59; W, 65.97. MW: 7776.53.

Tetra-*n*-butylammonium Salt (TBA3). Na3 (0.3 g, 0.4 mmol) was dissolved in 20 mL of H_2O and adjusted to pH = 4 by careful addition of 1 M HCl. Tetra-*n*-butylammonium (TBA) chloride (0.17 g, 0.62 mmol) was added with stirring. To the cloudy dark red solution was added 250 mL of CH_2Cl_2 . The mixture was shaken in a separatory funnel to obtain an almost colorless upper aqueous phase and a clear dark red lower organic layer. The organic layer was collected in a round-bottom flask and concentrated using a rotary evaporator. A reddish-brown solid was then precipitated from the concentrated organic layer by addition of diethyl ether as described above (0.33 g, yield 80%). The spectroscopic properties establish that **3** had not changed during the conversion of Na3 to TBA3. IR (2% KBr pellet, 1300–400 cm^{-1}): 1151 (w), 1087 (s), 1063 (w, sh), 1014 (w, sh), 943 (s), 909 (m), 887 (m), 830 (m), 783 (m), 744 (w), 691 (s), 530 (m), and 479 (w). ^{31}P NMR (9 mM solution in CH_3CN): two peaks for two symmetry-inequivalent distal P atoms at -7.6 ($\Delta\nu_{1/2} = 250$ Hz) and -11.0 ppm ($\Delta\nu_{1/2} = 180$ Hz). Anal. Calcd for $\text{C}_{256}\text{H}_{584}\text{Co}_3\text{Fe}_2\text{N}_{16}\text{O}_{112}\text{P}_4\text{W}_{28}$: C, 27.36; H, 5.24; Co, 1.57; Fe, 0.99; N, 1.99; P, 1.10; W, 45.80. Found: C, 27.73; H, 5.34; Co, 1.50; Fe, 1.02; N, 2.04; P, 1.05; W, 45.73. MW: 11239.68.

X-ray Crystallographic Structure Determination of Na2. A suitable crystal of **2** was coated with Paratone N oil, suspended on a small fiber loop, and placed in a cooled nitrogen gas stream at 100 K on a Bruker D8 SMART APEX CCD sealed-tube diffractometer with graphite-monochromated Mo K α (0.71073 Å) radiation. A sphere of data was measured using a series of combinations of ϕ and ω scans with 10 s frame exposures and 0.3° frame widths. Data collection, indexing, and initial cell refinements were all handled using SMART software.⁴⁷ Frame integration and final cell refinements were carried out using SAINT software.⁴⁸ The final cell parameters were determined from least-squares refinement on 8587 reflections. The SADABS program was used to carry out absorption corrections.⁴⁹

The structure was solved using direct methods and difference Fourier techniques (SHELXTL, V5.10).⁵⁰ All W, Fe, Cu, Na, and O(W) (O(W) is used to distinguish a water ligand from an oxygen atom) atoms were refined anisotropically, except for Na(19), Na(20), Na(21), and O(W)s 5, 6, 22, 23, and 29–42. Scattering factors and anomalous dispersion corrections are taken from the *International Tables for X-ray Crystallography*.⁵¹ Structure solution, refinement, graphics, and generation of publication materials were performed by using SHELXTL, V5.10 software.⁵⁰ Additional details of data collection and structure refinement are given in Table 1. At final convergence, R1 = 5.42% and GOF = 1.164 for 1212 parameters and 43097 data.

Catalytic Oxidation of Alkenes. In a typical alkene oxidation reaction, substrate (0.9 mmol) and TBA2 or TBA3 (0.004 mmol) were stirred under Ar at 25 °C in 1 mL of CH_3CN in a 10-mL Schlenk flask fitted with a Teflon stopcock and rubber stopper. The reaction was initiated by addition of 25 μL of 30% aqueous H_2O_2 . The organic products were identified and quantified by GC/MS and GC, respectively, using decane as the internal standard. The final H_2O_2 concentration was measured using standard iodometric analyses.⁵²

Table 1. Crystal Data and Structure Refinement for $\text{Na}_{16}\text{Cu}^{\text{II}}(\text{OH})_2\text{Fe}^{\text{III}}_2(\text{P}_2\text{W}_{15}\text{O}_{56})$ ($\text{P}_2\text{Cu}^{\text{II}}_2(\text{OH})_2\text{W}_{13}\text{O}_{52}$)

empirical formula	$\text{H}_0\text{Cu}_3\text{Fe}_2\text{Na}_{16}\text{O}_{142.75}\text{P}_4\text{W}_{28}$	
fw	8225.84	
temperature	100(2) K	
wavelength	0.71073 Å	
cryst syst	triclinic	
space group	$P\bar{1}$	
unit cell dimens	$a = 13.4413(9)$ Å	$\alpha = 80.475(2)^\circ$
	$b = 21.2590(15)$ Å	$\beta = 85.555(2)^\circ$
	$c = 25.5207(18)$ Å	$\gamma = 89.563(2)^\circ$
vol	$7170.2(9)$ Å ³	
Z	2	
density (calcd)	3.810 Mg/m ³	
abs coeff	23.192 mm ⁻¹	
reflns collected	96539	
indep reflns	43097 [R(int) = 0.0514]	
GOF on F^2	1.164	
final R indices [$I > 2\sigma(I)$]	R1 ^a = 0.0542, wR2 ^b = 0.1263	

$$^a R1 = \sum ||F_o| - |F_c|| / \sum |F_o|. \quad ^b wR2 = \{ \sum [w(F_o^2 - F_c^2)^2] / \sum [w(F_o^2)^2] \}^{0.5}$$

Results and Discussion

Synthesis. The complexes $[\text{TM}^{\text{II}}\text{Fe}^{\text{III}}_2(\text{P}_2\text{W}_{15}\text{O}_{56})(\text{P}_2\text{TM}^{\text{II}}_2\text{W}_{13}\text{O}_{52})]^{16-}$, TM = Cu (**2**) or Co (**3**), are readily prepared from the synthetic steps given in Figure 3. Reaction of $\alpha\text{-P}_2\text{W}_{15}\text{O}_{56}^{12-}$ with 2.0 equiv of FeCl_2 in 1 M NaCl solution followed by air oxidation produces $(\text{NaOH})_2\text{Fe}^{\text{III}}_2(\text{P}_2\text{W}_{15}\text{O}_{56})_2$, **1**, the prototype sandwich POM with α -junctions between the central unit and the trivacant POM units.⁴⁰ A 10-fold molar excess of the metal (Cu(II) or Co(II)) was added to increase the probability that the Na^+ centers would be fully replaced by these d-metal centers (the predicted structure was substitution of both Na^+ centers only). The complexes were crystallized from 0.5 M NaCl twice to remove any residual precursor metal complex and subsequently to form diffraction quality crystals. When excess Cu(II) or Co(II) is present, only an amorphous precipitate forms. In addition, the X-ray structures of Na2 and Na3 both show no uncoordinated Cu(II) or Co(II) atoms. The natural pH of **1** in unbuffered solution is ~ 6 . Addition of a ca. 10-fold molar excess of CuCl_2 or $\text{Co}(\text{NO}_3)_2$ relative to **1** lowers the pH of the solution to 3.9 or 5.6, respectively. The decrease in pH is most likely due to hydrolysis of aqua ligands on the metals in solution. This suggests that base hydrolysis of addenda W atoms may not be entirely responsible for the incorporation of the new metals in the belt of one of the $\alpha\text{-P}_2\text{W}_{15}$ fragments.⁵³ Cu(II) and Co(II) have distinctively different binding affinities for the POM complex. Cupric ion is readily incorporated into the POM structure at ambient temperature even when only a stoichiometric amount is present. ^{31}P NMR confirms that this reaction is quite selective as no other products are present within the detection limits of the instrument at these POM concentrations. In contrast, incorporation of Co(II) requires the sample to be heated (60 °C) at parity of reaction time (typically 2 min). ^{31}P NMR of the resulting solution established that the metal incorporation process is less selective than for Cu(II) (a mixture of products were present after addition of Co(II)). This was confirmed by cyclic voltammetry (*vide infra*).

One of the main goals of this work was to realize additional experimentally defensible synthetic methods for metal substitu-

(47) SMART, version 5.55; Bruker AXS, Inc., Analytical X-ray Systems: Madison, WI, 2000.

(48) SAINT, version 6.02; Bruker AXS, Inc., Analytical X-ray Systems: Madison, WI, 1999.

(49) Sheldrick, G. SADABS; University of Göttingen: Göttingen, 1996.

(50) SHELXTL, version 5.10; Bruker AXS, Inc., Analytical X-ray Systems: Madison, WI, 1997.

(51) *International Tables for X-ray Crystallography, Volume C*; Kynoch Academic Publishers: Dordrecht, 1992.

(52) Day, R. A., Jr.; Underwood, A. L. *Quantitative Analysis*, 5th ed.; Prentice Hall: Englewood Cliffs, NJ, 1986.

(53) Previous reports have shown that metal substitutions are possible in polyoxotungstates without first specifically generating a lacunary species, although these substitutions tend to be quite slow (on the order of months) ((a) Abbessi, M.; Contant, R.; Thouvenot, R.; Hervé, G. *Inorg. Chem.* **1991**, *30*, 1695–1702. (b) Jorris, T. L.; Kozik, M.; Casañ-Pastor, N.; Domaille, P. J.; Finke, R. G.; Miller, W. K.; Baker, L. C. W. *J. Am. Chem. Soc.* **1987**, *109*, 7402–7408).

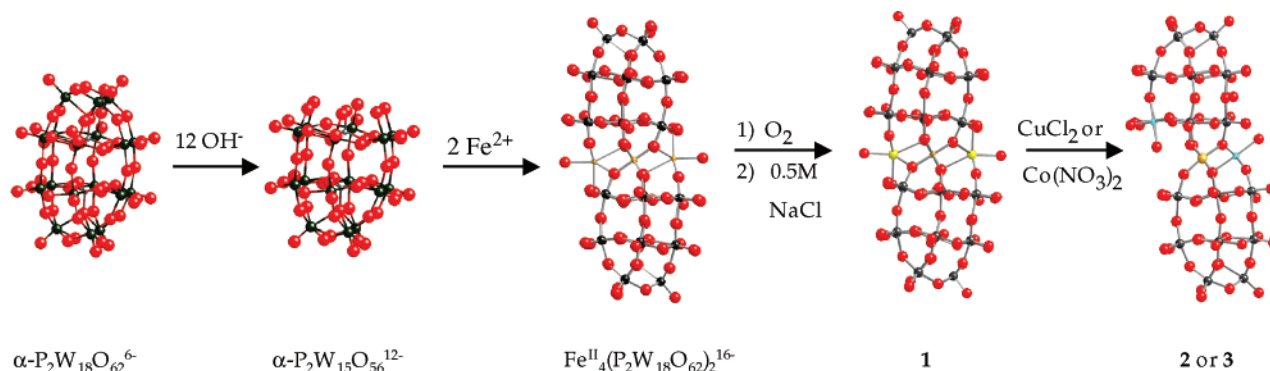


Figure 3. Synthesis of $[\text{TM}^{\text{II}}\text{Fe}^{\text{III}}_2(\text{P}_2\text{W}_{15}\text{O}_{56})(\text{P}_2\text{TM}^{\text{II}}\text{W}_{13}\text{O}_{52})]^{16-}$, where TM = Cu (**2**), Co (**3**). The structure of the $\text{Fe}^{\text{II}}_4(\text{P}_2\text{W}_{15}\text{O}_{56})_2$ intermediate was inferred by IR, ^{31}P NMR, and elemental analysis.

tion into sandwich-type POMs. Contant and co-workers developed a number of these techniques for POMs of the Wells–Dawson structural class. They determined that five factors govern the site-selective substitution of metals in cap and belt addenda positions of $\alpha\text{-P}_2\text{W}_{18-m-n}\text{V}_m\text{Mo}_n\text{O}_{62}^{(6+m)-}$. First, the reactivity of belt and cap addenda sites differs due to structurally distinct environments.⁵⁴ Second, the presence of a molybdenum atom in a belt site enhances the reactivity of the nearest cap site. Third, the presence of a vanadium atom in a belt site has a “directing effect” upon hydrolysis resulting in the selective departure of the W_3O_{13} cap in the half of the anion opposite the one containing vanadium; molybdenum has no such influence. Fourth, molybdenum is more labile than tungsten. Fifth, molybdenum and tungsten can be added stepwise to lacunary species; whereas, vanadium addition always results in a fully intact or “saturated” species. Our work now illustrates the effects of cap isomerization on substitution patterns in sandwich-type polyoxometalates. Traditional B-Keggin and Wells–Dawson sandwich-type POMs (i.e., those sandwich species having β -junctions linking trivalent POM units to the central unit) all show symmetric metal incorporations. Specifically, metal incorporation is limited to the central unit.^{34,55} Complexes **2** and **3**, however, provide examples of asymmetric metal incorporation involving not only the central unit but also only one of the two trivalent POM units.

The tetra-*n*-butylammonium (TBA) salts of **2** and **3** (TBA**2** and TBA**3**) were prepared by metathesis reactions. As in the preparation of the TBA salts of $\alpha\text{-P}_2\text{MW}_{17}\text{O}_{62}^{n-}$, control of pH is necessary. POM degradation is operable at too low or too high pH values. Complexes **2** and **3** are stable over a fairly wide pH range (pH = 1–6), and cation exchange (TBA⁺ for Na⁺) was possible in unbuffered solutions without formation of any degradation products as indicated by IR and elemental analyses. The TBA salts of **2** and **3** are soluble in a number of organic solvents including acetonitrile, acetone, and dichloromethane.

X-ray Crystallography of Na2. The X-ray crystal structure of Na**2** reveals an iron- and copper-containing polytungstophosphate sandwich-type POM with a novel structural motif. Figure 4 and Table 1 summarize the structural data on Na**2**. As

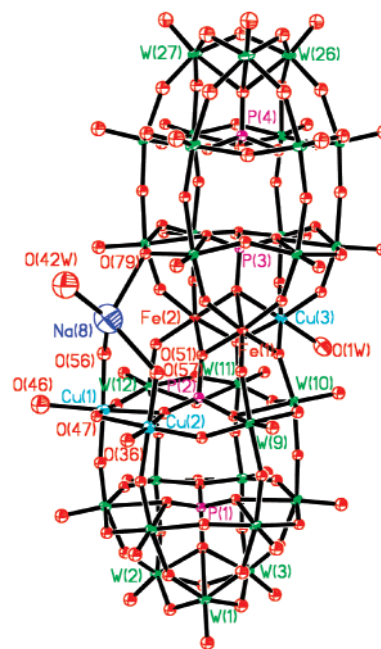


Figure 4. Thermal ellipsoid plot (50% probability surfaces) of the polyanion $\text{Na}(\text{OH}_2)(\text{Cu}^{\text{II}}(\text{OH}_2)\text{Fe}^{\text{III}}_2(\text{P}_2\text{W}_{15}\text{O}_{56})(\text{P}_2\text{Cu}^{\text{II}}_2(\text{OH}_2)_4\text{W}_{13}\text{O}_{52}))^{16-}$ (Na**2**). All appropriate atom labels are given. All but one of the Na cations (Na8) are omitted for clarity. The bond lengths of Na(8)–O(42W), Cu(1)–O(46), Cu(1)–O(56), Cu(2)–O(36), and Fe(1)–O(51) are 2.80(3), 2.296(11), 2.055(10), 2.127(9), and 2.045(8) Å, respectively. The bond angles of O(57)–Na(8)–O(42W), O(56)–Cu(1)–O(46), and P(2)–O(51)–Fe(1) are 111.1(8)°, 86.2(4)°, and 124.2(4)°, respectively.

shown in Figure 4, the structure of **2** consists of a single defect Fe_2Cu unit sandwiched between two substitutionally distinct Wells–Dawson moieties. As in **1**, the linkage between the trivalent POM unit (at the site of Cu incorporation) and the central Fe_2Cu unit in **2** is rotated 60° relative to that in all known B-Keggin and Wells–Dawson sandwich-type POMs. Significantly, this indicates that the inter-POM-unit connectivity (the α -junction) is maintained at the site of metal incorporation and only at this site.

Several other structural features merit additional discussion. First, Cu(II) centers have replaced the two tungsten atoms located in the adjacent belt region on the side of the POM opposite the metal substitution site of the central unit (the site containing the Cu^{II}), while the other P_2W_{15} unit remains intact. Interestingly, pronounced Jahn–Teller distortion is only seen in the $\text{Cu}^{\text{II}}\text{O}_5(\text{OH}_2)$ octahedron in the central unit. This octahedron shows elongation of the axial Cu–O bond analogous to that seen in other $\text{Cu}^{\text{II}}\text{O}_6$ -containing sandwich-type POMs.¹⁹ In contrast, the two $\text{Cu}^{\text{II}}\text{O}_4(\text{OH}_2)_2$ octahedra found in the belt

(54) Comparison of the cyclic voltammograms of isomerically pure α_1 - and α_2 - $\text{Fe}(\text{OH}_2)\text{P}_2\text{W}_{17}\text{O}_{61}^{7-}$ confirms the influence of the location of the iron-filled site on the electrochemical properties of the molecules. The authors attribute these differences to framework distortion in the α_1 isomer and the subsequent variations in protonation that follow. This distortion favors the coalescence of waves in the cyclic voltammograms (Contant, R.; Abbessi, M.; Canny, J.; Belhouari, A.; Keita, B.; Nadjo, L. *Inorg. Chem.* **1997**, *36*, 4961–4967).

(55) Neumann, R.; Khenkin, A. M. *Inorg. Chem.* **1995**, *34*, 5753–5760.

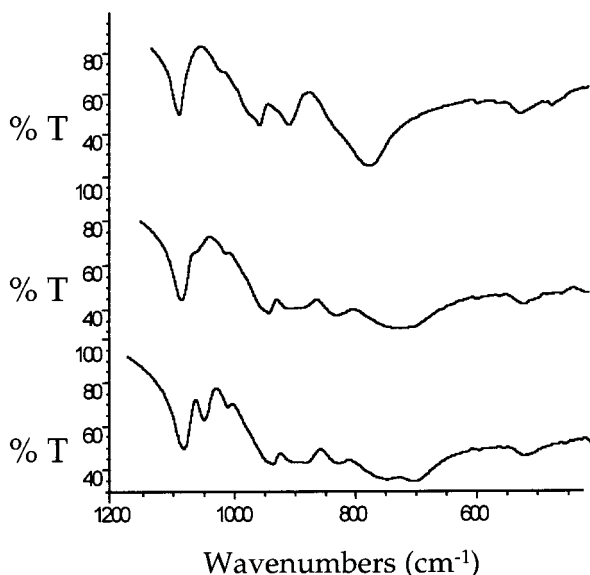


Figure 5. Infrared spectra of α -K₆P₂W₁₈O₆₂ (top), Na₁₆Cu^{II}(OH₂)Fe^{III}₂-(P₂W₁₅O₅₆)(P₂Cu^{II}₂(OH₂)₄W₁₃O₅₂) (Na₂) (middle), and Na₁₆(NaOH)₂-Fe^{III}₂(P₂W₁₅O₅₆)₂ (Na₁) (bottom). Spectra were run by adding 2% sample to KBr, forming a pellet, and collecting data from 1300 to 400 cm⁻¹.

sites of the P₂W₁₃ unit show no pronounced distortion. Second, there is a vacancy left in the central unit (effectively creating an M₃ central unit) where a Na⁺ is very loosely coordinated to the complex. This Na⁺ connects the POM to the neighboring POM in the adjoining unit cell. This is the first Wells–Dawson-type structure to have two belt tungsten atoms replaced by early transition metals with no simultaneous replacement of cap tungsten atoms. Simultaneous metal replacements are exemplified by the hydrolysis and metal reconstitution chemistry of the hexavacant Wells–Dawson POMs.^{1,56,57} Finally, these are the first Wells–Dawson-derived sandwich structures to have more than one type of transition metal in the central unit analogous to that seen in the Keggin-type polytungstozincate sandwich POMs first prepared by Tourné and co-workers.³⁴

To establish that the formation and isolation of **2** was not fortuitous, but rather represented entry into a new family of mixed-metal sandwich-type POMs, a low resolution (R1 ~ 15%) X-ray structure of Na₃ was solved (see Supporting Information). The crystals of Na₃ were of poorer quality than those of Na₂, so details of the disordered solvent water molecules and sodium ions could only be determined semiquantitatively. The overall *R* value reflects this disorder. Nonetheless, the structure of the polyanion unit, **3**, per se, was still well determined and is isostructural with **2**.

Physical Properties. Figure 5 shows the IR spectra of **2** along with the parent Wells–Dawson structure (α -K₆P₂W₁₈O₆₂) and the precursor iron sandwich complex, **1**. The ν_3 vibrational mode of the central PO₄ unit in **1** is split (1089 and 1062 cm⁻¹) more than in **2** (1088 and 1062 cm⁻¹), implying that the structural distortion of this central PO₄ unit is higher (and the force field less symmetric) in **1** than in **2**.⁵⁸ The W–O stretching frequencies (from 900 to 500 cm⁻¹) also show additional peaks relative to the parent Wells–Dawson structure. Especially noteworthy is the enhanced splitting of the strong peaks centered around

800 cm⁻¹ in **2** relative to the parent iron sandwich complex, **1**. This is the only indication in the spectra that changes in the polyoxotungstate framework have taken place as all other peaks are nearly a band-for-band match with **1** (within experimental error). The electronic spectra of **2** and **3** are not structurally informative. The intense oxygen-to-metal-charge-transfer bands exhibited by all POMs obscure the Fe-centered and Cu- or Co-centered d–d transitions for complexes **2** and **3**, respectively. The ³¹P NMR spectra of **2** and **3** both show two singlets for the symmetry-inequivalent P atoms distal to the Fe₂Cu and Fe₂Co centers, respectively. Like most other Wells–Dawson-type TMSPs, the peaks due to the P atoms proximal to the paramagnetic d-electron centers are too broad to be observed.⁵⁹ For the copper complex, **2**, one fairly broad peak appears at –11.2 ppm ($\Delta\nu_{1/2}$ = 300 Hz) while the other broad peak appears at –10.0 ppm ($\Delta\nu_{1/2}$ = 350 Hz). These peaks are assigned to the distal P atoms in the P₂Cu₂W₁₃ and P₂W₁₅ units, respectively.⁵⁹ The cobalt complex, **3**, has one peak at –16.5 ppm ($\Delta\nu_{1/2}$ = 75 Hz), while the other peak appears at –10.2 ppm ($\Delta\nu_{1/2}$ = 130 Hz). These peaks are assigned to the distal P atoms in the P₂Co₂W₁₃ and P₂W₁₅ units, respectively.⁵⁹ As expected, the shifts of the distal P atom in the P₂W₁₅ units of **2** and **3** should be similar since these units are virtually identical structurally in these two complexes. Literature precedence shows that early transition metal substitutions in the POM unit result in upfield shifts for the distal P atoms with the effects more pronounced for α_2 isomers than α_1 (cap W atom replacement versus belt W atom replacement).⁵⁹ The magnetic moments of **2** and **3** are 9.9 and 11.7 μ_B , respectively, at 24 °C, which implies some degree of antiferromagnetic coupling. The theoretical spin-only magnetic moments are 14 and 20 μ_B for ferromagnetically coupled *S* = 6.5 and 9.5 systems, respectively. This is consistent with some narrowing of the peaks in the spectra of **2** and **3** relative to the parent complex, **1**.

Electrochemistry. The electrochemical properties of the parent diferric complex, **1**, have been studied along with the Cu and Co derivatives (**2** and **3**, respectively). The preliminary results are presented here. Future work will focus more closely on the redox properties of these complexes in connection with their catalytic properties. Although the electrochemical characterization of a diferric polytungstophosphate is lacking in the literature, Song and co-workers⁶⁰ reported that the tetraferroc sandwich-type POM, Fe₄(P₂W₁₅O₅₆)₂¹²⁻, exhibits one simple one-electron reduction, one four-electron reduction, and one two-electron reduction. Figure 6 presents the cyclic voltammograms of the diferric parent complex, **1** (Figure 6A), along with a comparison with its Cu²⁺ (Figure 6B,C) and Co²⁺ derivatives (Figure 6D). The diferric parent complex, **1**, exhibits one broad ill-defined wave at *E*_{pc} = –260 mV (corresponding oxidation potential at *E*_{pa} = –100 mV) and two well-defined reduction potentials at *E*_{pc} = –680 mV and *E*_{pc} = –956 mV (corresponding oxidation potentials at *E*_{pa} = –500 mV and *E*_{pa} = –615 mV, respectively). On the basis of literature precedence, the first wave is most likely attributed to the reduction of the Fe³⁺ centers, while the other two waves can be assigned to the reduction of the polyoxotungstate skeleton.⁶¹

The cyclic voltammograms of the Cu²⁺-substituted complex, **2** (Figure 6B,C), show the presence of a redox process not seen in the parent complex, **1**. This is attributed to the Cu²⁺/Cu¹⁺

(56) Contant, R.; Tézé, A. *Inorg. Chem.* **1985**, *24*, 4610–4614.

(57) Judd, D. A.; Chen, Q.; Campana, C. F.; Hill, C. L. *J. Am. Chem. Soc.* **1997**, *119*, 5461–5462.

(58) Rocchiccioli-Deltcheff, C.; Thouvenot, R. *J. Chem. Res., Synop.* **1977**, 46–47.

(59) Jorris, T. L.; Kozik, M.; Casañ-Pastor, N.; Domaille, P. J.; Finke, R. G.; Miller, W. K.; Baker, L. C. W. *J. Am. Chem. Soc.* **1987**, *109*, 7402–7408.

(60) Song, W.; Wang, X.; Liu, Y.; Liu, J.; Xu, H. *J. Electroanal. Chem.* **1999**, *476*, 85–89.

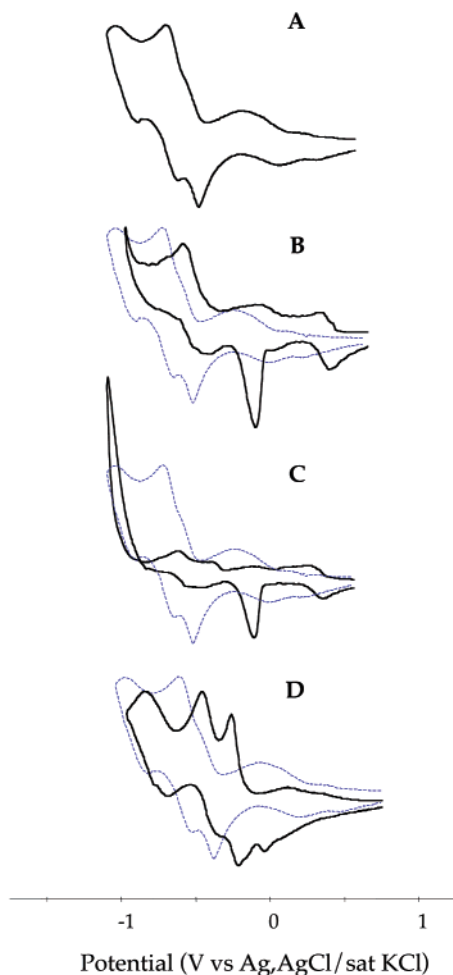


Figure 6. Cyclic voltammograms: (A) 0.5 mM **1**; (B) 0.5 mM **2** (solid line) and 0.5 mM **1** (dashed line) shown from -0.8 to 0.8 V; (C) 0.5 mM **2** (solid line) and 0.5 mM **1** (dashed line) shown from -1.0 to 0.8 V; (D) 0.5 mM **3** (solid line) and 0.5 mM **1** (dashed line).

couple, and it is consistent with previously reported values.^{62–64} In addition, several waves present in both **1** and **2** are now shifted to more positive potentials in **2**. The cyclic voltammogram of the Co^{2+} -substituted complex, **3**, differs significantly

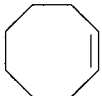
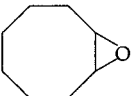
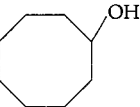
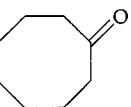
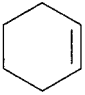
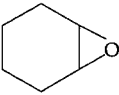
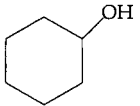
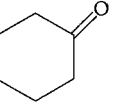
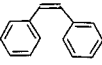
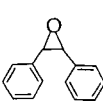
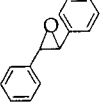
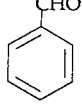
(61) Very similar behavior is found in the voltammograms of $\alpha_2\text{-P}_2\text{-Fe}^{\text{III}}\text{W}_{17}\text{O}_{61}^{7-}$ ((a) Contant, R.; Abbessi, M.; Canny, J.; Belhouari, A.; Keita, B.; Nadjo, L. *Inorg. Chem.* **1997**, *36*, 4961–4967. (b) Keita, B.; Belhouari, A.; Nadjo, L.; Contant, R. *J. Electroanal. Chem.* **1998**, *442*, 49–57.). These investigators found that the first reduction wave of $\alpha_2\text{-P}_2\text{-Fe}^{\text{III}}\text{W}_{17}\text{O}_{61}^{7-}$, which is exactly half as intense as the first reduction of **1**, involves the consumption of ca. 1.8 electrons per molecule and should be ascribed in part to $\text{Fe}(\text{III}) + e^- \rightarrow \text{Fe}(\text{II})$ and in part to $2\text{W}(\text{VI}) + 2e^- \rightarrow 2\text{W}(\text{V})$ (reduction of the polyoxotungstate skeleton).

(62) (a) Keita, B.; Lu, Y. W.; Nadjo, L.; Contant, R.; Abbessi, M.; Canny, J.; Richet, M. *J. Electroanal. Chem.* **1999**, *477*, 146–157. (b) Keita, B.; Girard, F.; Nadjo, L.; Contant, R.; Canny, J.; Richet, M. *J. Electroanal. Chem.* **1999**, *478*, 76–82. (c) Keita, B.; Abdelljalil, E.; Nadjo, L.; Avisse, B.; Contant, R.; Canny, J.; Richet, M. *Electrochem. Commun.* **2000**, *2*, 145–149.

(63) Reduction of the Cu-containing POM, **2**, results initially in deposition of Cu(0) on the electrode surface, and subsequently (upon reoxidation) in an anodic stripping peak not observed in the Co-containing POM, **3**.

(64) The cyclic voltammograms of **2** show two other interesting processes. First, the desorptive oxidation wave with $E_{\text{pa}} = -164$ mV is characteristic of the deposition of copper on the electrode surface during the reduction process. Second, the fourth reduction wave at $E_{\text{pc}} = -990$ mV has a very large current intensity (most pronounced when the potential is carried to -1000 mV, as in Figure 6C). On the basis of literature precedence, this is most likely attributable to a hydrogen evolution reaction (see ref 62).

Table 2. Product Distributions for Ambient Temperature Oxidation of Alkenes by H_2O_2 Catalyzed by TBA2 and TBA3^a

Substrate (Catalyst)	Products Selectivity (Yields Based on H_2O_2) [Turnovers] ^b			
				
(TBA2)	86%(79%)[14]	0 ^c	11%[1]	
(TBA3)	94%(90%)[14]	3%[0.4]	3%[0.5]	
				
(TBA2)	19%(18%)[1]	11%[0.6]	70%[4]	
(TBA3)	11%(8%)[1]	33%[3]	56%[5]	
				
(TBA2)	89%(66%)[8]	11%(6%)[1]	0 ^c	
(TBA3)	89%(64%)[8]	11%(6%)[1]	0 ^c	

^a Conditions: 25 μL of 30% $\text{H}_2\text{O}_2(\text{aq})$ was injected into 1 mL of CH_3CN 4 mM in TBA2 or TBA3 and 0.9 M in alkene under Ar to initiate the reaction. Organic products were quantified by GC and GC/MS. ^b Selectivity = (moles of indicated product/moles of all organic products derived from the substrate) \times 100; epoxide yields based on peroxide consumed = (moles of epoxide/moles of H_2O_2 consumed) \times 100 turnovers = moles of indicated product/moles of catalyst after 30 h reaction time. ^c No products within the detection limit ($<0.2\%$).

from those of both **1** and **2** (Figure 6D). As in **2**, all of the voltammetric peaks in **3** are shifted to more positive potentials relative to those in the diferric parent complex, **1**.

There are three lines of evidence consistent with the Cu^{2+} oxidation state in **2**: First, **2** is prepared with Cu^{2+} as the only Cu source, and reduction of Cu^{2+} to Cu^+ is unlikely in the synthetic medium. Second, bond-length-based valence sum calculations from the X-ray structure of Na**2** yield an average oxidation state of 2.02 ± 0.04 .^{65–67} Third, the charge requirements for the anions and cations of Na**2** are most consistent with Cu^{2+} .

Catalysis. In a typical reaction, 0.9 mmol of alkene was added to 1.0 mL of acetonitrile containing 4.00 μmol of POM. The reaction was initiated by the addition of 25 μL of 30% aqueous H_2O_2 . The alkene-derived product distributions for the oxidation of representative alkenes are given in Table 2. The selectivities for epoxide with the alkenes cyclooctene and *cis*-stilbene are reasonably high, which rules out homolytic processes (e.g., Fe-initiated radical chain processes) as the dominant mechanism.^{68,69} In contrast, TBA2 and TBA3 are inefficient as catalysts for cyclohexene oxidation. Furthermore, both the

(65) Brown, I. D. In *Structure and Bonding in Crystals*; O'Keefe, M., Navrotsky, A., Eds.; Academic Press: New York, 1980; Vol. 2.

(66) Brown, I. D. *VALENCE*, version 2.0; Brockhouse Inst. Materials Res., McMaster University: Hamilton, ON, Canada, 1996.

(67) Brown, I. D.; Altermatt, D. *Acta Crystallogr.* **1985**, *B41*, 244–247.

(68) Sheldon, R. A.; Kochi, J. K. *Metal-Catalyzed Oxidations of Organic Compounds*; Academic Press: New York, 1981.

(69) Hill, C. L.; Khenkin, A. M.; Weeks, M. S. *ACS Symp. Ser.* **1993**, *523*, 67–80.

selectivities and activities for all substrates catalyzed by TBA2 and TBA3 were less than for TBA1, indicating that metal incorporation does have a substantial impact. The degree of H₂O₂ disproportionation catalyzed by TBA2 and TBA3 was quantified by iodometric titration.⁶⁸ Unlike many other previously reported Fe-containing POMs (except TBA1⁴⁰ and γ -[Si-(FeOH)₂W₁₀O₃₈]⁶⁻^{70,71}), the organic product yields based on H₂O₂ consumption are high for some alkenes as indicated in Table 2. Like many of their TMSP predecessors, TBA2 and TBA3 are very stable at high H₂O₂ concentrations (no apparent structural degradation after 72 h in 0.24 M H₂O₂) on the basis of IR, elemental analysis, and ³¹P NMR.

Conclusions. Metal incorporation (Cu²⁺ or Co²⁺) into the framework of the diferric sandwich-type POM, (NaOH)₂Fe^{III}₂(P₂W₁₅O₅₆)₂ (**1**), in aqueous solution results in the formation of complexes **2** or **3**, respectively. The X-ray crystal structures of Na2 and Na3 reveal new Fe- and Cu- or Co-containing polytungstophosphate sandwich-type POMs that maintain the inter-POM-unit connectivity first seen in **1** at the site of metal incorporation. These complexes show unique asymmetric substitution patterns for the incorporation of d-metal centers not

seen in other sandwich structures. These metal incorporation patterns are attributed to differences in the inter-POM-unit connectivity since all other B-Keggin and Wells–Dawson sandwich POMs show symmetric metal incorporations (with metal incorporation limited to the central unit). Complexes **2** and **3** show substitution patterns, which involve not only the central unit, but also the α_1 (belt) sites in only one of the trivacant POM units. Copper or cobalt addition into the framework of **1** results in a substantial perturbation of the electrochemical properties of the polyoxotungstate framework. The tetra-*n*-butylammonium salts of **2** and **3**, which are readily prepared by metathesis, are stable and catalyze the epoxidation of cyclooctene and *cis*-stilbene with high selectivity and high yields based on H₂O₂.

Acknowledgment. We thank the ARO (Grant DAAG55-98-1-0251) and NSF (Grant CHE-9975453) for support. We also thank Michelle Ritorto and Wade Neiwert for assistance with the manuscript. This paper is dedicated to Dr. Van H. Crawford of Mercer University in Macon, Georgia, on the occasion of his retirement.

Supporting Information Available: Crystallographic data in CIF format for both Na2 and Na3. This material is available free of charge via the Internet at <http://pubs.acs.org>.

IC0105314

(70) Nozaki, C.; Kiyoto, I.; Minai, Y.; Misono, M.; Mizuno, N. *Inorg. Chem.* **1999**, *38*, 5724–5729.

(71) Mizuno, N.; Nozaki, C.; Kiyoto, I.; Misono, M. *J. Catal.* **1999**, *182*, 285–288.